Polymer 51 (2010) 2390–2402

Contents lists available at ScienceDirect

Polymer

journal homepage: www.elsevier.com/locate/polymer

# Main chain and segmental dynamics of semi interpenetrating polymer networks based on polyisoprene and poly(methyl methacrylate)

Jacob John [a,*], Damir Klepac [b], Mirna Didović [b], C.J. Sandesh [c], Yong Liu [d], K.V.S.N. Raju [e], Anitha Pius [a], Srećko Valić [b,f,**], Sabu Thomas [g,***]

[a] Department of Chemistry, Gandhigram Rural University, Dindigul, Tamil Nadu 624302, India
[b] Department of Chemistry and Biochemistry, School of Medicine, University of Rijeka, Braće Branchetta 20, 51000 Rijeka, Croatia
[c] NMR Research Center, Indian Institute of Science, Bangalore 560012, India
[d] College of Mechanical and Electrical Engineering, Beijing University of Chemical Technology, Beijing 100029, China
[e] Division of Organic Coatings and Polymers, Indian Institute of Chemical Technology, Hyderabad 500607, India
[f] Rudjer Bošković Institute, Bijenička 54, 10000 Zagreb, Croatia
[g] School of Chemical Sciences, Mahatma Gandhi University, P. D. Hills, Kerala 686560, India

ARTICLE INFO

*Article history:*
Received 29 October 2009
Received in revised form
11 March 2010
Accepted 13 March 2010
Available online 24 March 2010

*Keywords:*
Semi IPN
Chain dynamics
Spin resonance

ABSTRACT

Main chain and segmental dynamics of polyisoprene (PI) and poly(methyl methacrylate) (PMMA) chains in semi IPNs were systematically studied over a wide range of temperatures (above and below $T_g$ of both polymers) as a function of composition, crosslink density, and molecular weight. The immiscible polymers retained most of its characteristic molecular motion; however, the semi IPN synthesis resulted in dramatic changes in the motional behavior of both polymers due to the molecular level interpenetration between two polymer chains. ESR spin probe method was found to be sensitive to the concentration changes of PMMA in semi IPNs. Low temperature spectra showed the characteristics of rigid limit spectra, and in the range of 293–373 K, complex spectra were obtained with the slow component mostly arising out of the PMMA rich regions and fast component from the PI phase. We found that the rigid PMMA chains closely interpenetrated into the highly mobile PI network imparts motional restriction in nearby PI chains, and the highly mobile PI chains induce some degree of flexibility in highly rigid PMMA chains. Molecular level interchain mixing was found to be more efficient at a PMMA concentration of 35 wt.%. Moreover, the strong interphase formed in the above mentioned semi IPN contributed to the large slow component in the ESR spectra at higher temperature. The shape of the spectra along with the data obtained from the simulations of spectra was correlated to the morphology of the semi IPNs. The correlation time measurement detected the motional region associated with the glass transition of PI and PMMA, and these regions were found to follow the same pattern of shifts in α-relaxation of PI and PMMA observed in DMA analysis. Activation energies associated with the $T_g$ regions were also calculated. $T_{50G}$ was found to correlate with the $T_g$ of PMMA, and the volume of polymer segments undergoing glass transitional motion was calculated to be 1.7 $nm^3$. C-13 $T_{1\rho}$ measurements of PMMA carbons indicate that the molecular level interactions were strong in semi IPN irrespective of the immiscible nature of polymers. The motional characteristics of H atoms attached to carbon atoms in both polymers were analyzed using 2D WISE NMR. Main relaxations of both components shifted inward, and both SEM and TEM analysis showed the development of a nanometer – sized morphology in the case of highly crosslinked semi IPN.

## 1. Introduction

Interpenetrating polymer networks, IPNs, are a combination of two or more polymers in network form, with at least one such polymer polymerized and/or crosslinked in the immediate presence of the other(s). The idea is to effect a molecular interpenetration of the networks; in practice, most IPNs form immiscible compositions, usually phase separating during some

---

* Corresponding author. Tel.: +1 213 707 0026.
** Corresponding author at: Department of Chemistry and Biochemistry, School of Medicine, University of Rijeka, Braće Branchetta 20, 51000 Rijeka, Croatia. Tel.: +385 51651134; fax: +385 51651135.
*** Corresponding author. Tel.: +91 481 2730003.
*E-mail addresses:* jacobparayil@gmail.com (J. John), valics@medri.hr (S. Valić), sabuchathukulam@yahoo.co.uk (S. Thomas).

0032-3861/$ – see front matter © 2010 Elsevier Ltd. All rights reserved.
doi:10.1016/j.polymer.2010.03.025

stage of synthesis. The IPNs are part of the broad class of polymer blends [1–3]. The properties of these materials strongly depend on phase morphology and polymer chain dynamics. In semi IPN, we combine the useful properties of both polymers and overcome the drawbacks of individual components when they form blends. During this process, the molecular chain dynamics, which determine the properties of these polymers, change dramatically and this change depends on the level of mixing between two polymers. The change is more pronounced when we combine an elastic polymer with a glassy one. ESR spin probes have been widely used to obtain information about motional behavior and relaxation processes in polymers [4–7]. These reporters are paramagnetic species, commonly stable nitroxide radicals, which are dispersed (spin probes) or covalently attached to the polymer matrix (spin labels). The electron spin resonance (ESR) spectrum of the nitroxide radical is a function of its rotational motion and is sensitive to the nitroxide mobility, with correlation times ($\tau_c$) in the range $10^{-7}$ - $10^{-11}$s. Numerous studies have indicated that the mobility of the nitroxide radical is related to the dynamics of the host polymer [8–11].

ESR spin probes reflect different environments in a given sample if the respective rates of motion are different [10–12]. If the nitroxide molecules are located in both phases of the heterogeneous two-component polymer system, the ESR spectra are composed of two components differing in their correlation times. A wide range of molecular motions can be studied, including those of very slow motion characteristics for polymers well below glass transition temperature, $T_g$, and those of fast motion (above $T_g$). The nitroxide rotational correlation times ($\tau_c$) can be determined reliably from the experimentally observed ESR line shapes, which retains many of the features observed from a collection of randomly oriented immobilized or/moving nitroxide molecules, $\tau_c$ thus provides valuable information about segmental dynamics and phase separation in IPN systems [11,12].

Measurement of carbon spin-lattice relaxation in rotating frame ($T_{1\rho}$) could give information on the local mobility of polymer chains and therefore usually are employed to investigate the effect of blending on the local motions in a polymer blend. C-13 $T_{1\rho}$ relaxation times are sensitive to molecular motions with frequencies of ca. 10–100 kHz. Spin diffusion between C-13 nuclei is slow compared with H-1 spin diffusion, especially under condition of magic angle spinning. Therefore C-13 $T_{1\rho}$ relaxation times are not partially averaged by spin diffusion as are proton $T_{1\rho}$ relaxation times, and therefore information on the motion of each specific site is retained [13–15].

The wideline separation (WISE) NMR was introduced some years ago as a simple and elegant method to measure chain dynamics of polymers by correlating the proton line shape with the carbon chemical shift. This experiment yields information about the dynamics by measuring the degree to which the proton line shapes are averaged by molecular motion [16–18]. The present study aims to investigate the motional characteristics of polymer chains as a function of temperature, intermolecular interactions that affect the molecular motion and miscibility using ESR spin probe method, solid state NMR and DMA. The ESR spectra obtained were found to be morphology sensitive and display temperature and structure dependent anisotropic rotation of spin probe. In this report we compare the ESR results deduced from the spin probe measurements to those obtained from DMA and solid state NMR measurements. The effects of composition, crosslink density and molecular weight on chain dynamics are also analyzed. ESR line shapes and spectral simulation data are used to arrive at some morphological conclusions along with the help of SEM and TEM.

## 2. Experimental section

### 2.1. Materials

High molecular weight polyisoprene (PI) ($M_w \sim 500{,}000$) was supplied by Rubber Research Institute of India (RRII). Low molecular weight PI ($M_w \sim 40{,}000$) was purchased from Aldrich. Cross-linker for the PI, Dicumyl Peroxide (DCP 99%) was purchased from Aldrich and used as such. Methyl methacrylate (MMA, Aldrich) was distilled under vacuum prior to use. AIBN (Aldrich) was purified by recrystallization from methanol. The probe 4-hydroxy-2,2,6,6-tetramethylpiperidine-1-oxyl (TEMPOL) was obtained from Aldrich.

### 2.2. Preparation of semi IPNs

Cross-linked polyisoprene sheets (1–2 mm thick) were weighed and kept immersed in a homogeneous mixture of methyl methacrylate and AIBN (0.7 g per 100 g of MMA). The PI sheets were swollen at different time intervals to obtain different weight percentages of PMMA. The swollen samples were kept at 0 °C for a few hours to achieve equilibrium distribution of the MMA monomer in the matrix. These swollen networks were heated at 353 K for 6 h and at 373 K for 2 h in an atmosphere of MMA to complete the polymerization of MMA (PMMA $M_w = 733{,}000$ g/mol and PDI = 3.09 from GPC). The obtained semi IPNs were kept in a vacuum air oven to make it free of unreacted MMA. The final weight of the IPN was taken and composition of the sample was determined. The pure polyisoprene was given the name sample Z and others are sometimes designated as follows, PI/PMMA 65/35 as M, 50/50 (2% crosslinker) as H, 50/50 (4% crosslinker) as O, and 50/50 low molecular wt. sample as W ($^a$NRM$_b$, a – crosslinker conc., b – PMMA conc.)

### 2.3. Electron spin resonance (ESR) measurements

The free nitroxide radical 4-hydroxy - 2,2,6,6, - tetramethylpiperidine-1-oxyl (TEMPOL) was used as spin probe for ESR measurements. TEMPOL was chosen to study the investigated semi IPNs since this spin probe was successfully used earlier for the study of natural rubber and similar systems [12]. The probe molecules were incorporated into tiny semi IPN samples by swelling the samples in probe solution. The temperature was kept constant (308 K) during three days of the probe incorporation process. Throughout this period, the probe molecules diffuse into swollen semi IPN networks. At the same time, the solvent was slowly removed from the solution by evaporation. However, a small amount of the solvent usually stays trapped in the higher density regions of PI samples. For that reason, the samples were annealed in vacuum at 333 K and weighed from time to time. When their masses remained unchanged as a function of annealing time, the residual solvent was completely removed. The total amount of probe molecules in the samples was 0.15 wt.%.

ESR measurements were performed on a Varian E–109 spectrometer operating at 9.2 GHz, equipped with a Bruker ER 041 XG microwave bridge and a Bruker ER 4111 VT temperature unit. Spectra were recorded in a wide temperature range from 173 K to 413 K in steps from 5 to 10 K depending on the sensitivity of spectral line changes within each temperature region. The rigid limit spectra were recorded at 100 K for all samples. The samples were kept at the temperature of measurement at least 10 min before the accumulation started. EW (EPRWare) Scientific Software Service program was used for data accumulation and manipulation. The number of accumulations varied from 2 to 5 depending on signal to noise ratio.

### 2.4. Dynamic mechanical analysis (DMA)

Dynamic mechanical Analyses were performed in a Rheometrics DMA IV. Measurements were conducted at a frequency of 1 Hz from 188 K to 443 K at a heating rate of 3 K per minute.

### 2.5. C-13 $T_{1\rho}$ relaxation measurements

Solid state $^{13}C$ – CPMAS NMR spectra were recorded on a Bruker 300 MHz spectrometer, operating at a 75.46 MHz frequency for C-13 nuclei. Samples were spun at spinning speed of 3.1 kHz. The 90° pulse time was 4.5 μs, corresponding to a spin-locking field strength of 40 kHz. C-13 $T_{1\rho}$ measurements were made by applying a C-13 spin-locking pulse after a 2 ms CP preparation period. The decay of the C-13 magnetization in the spin-locking field was followed for spin-locking times of up to 14 ms.

### 2.6. 2D-WISE NMR

We used pulse sequence developed by Schmidt-Rohr et al. to obtain 2D WISE spectra [16]. The pulse sequence consists of a 90° *x* pulse, which flips the magnetization into the *xy* plane, followed by a $t_1$ evolution period. Next a 90°–*x* pulse is applied to flip the magnetization back to *z*-axis. The magnetization was then allowed to diffuse during a constant mixing period ($t_m$), which ranged from 100 μs to 50 ms. After the mixing period another 90° *x* pulse flips the $^1H$ magnetization back into transverse plane where it is immediately subjected to cross-polarization from protons to carbons.

### 2.7. SEM and TEM analysis

Scanning Electron Microscopy (SEM) analyses were performed with a JEOL JSM 6320F Field Emission Gun Scanning Electron Microscope. The samples were cryofractured and surface of semi IPN is coated with Platinum using a Gatan HR 681 Ion Beam Coater. Transmission electron microscopy analyses were performed on a Hitachi H-800 TEM instrument. Ultra thin films were made using cryomicrotome and $OsO_4$ was used to dye the PI phase.

## 3. Results and discussion

### 3.1. Spin probe ESR measurements

ESR spectra of the spin probes in semi IPNs with different composition, crosslink density and molecular weight were measured in the temperature range of 173 K–413 K at intervals of 10 K or less. Selected spectra are shown in Fig. 1(a) for the spin probed PI. The temperature dependence of spectra is due to changes in rotational rate of the nitroxide radical, characterized by the correlation time ($\tau_c$). In ESR experiments, two motional regimes are usually detected, one corresponds to slow motional spectra with correlation times in the range of $10^{-7}$–$10^{-9}$ s and the other one is the "averaged" or motionally narrowed spectra, with $\tau_c$ in the range of $10^{-9}$–$10^{-11}$ s.

The spectra of pure crosslinked PI in Fig. 1(a) shows the characteristic of natural rubber having a sol–gel composition. The spin probe reflects composite ESR spectra at low temperatures (around 273 K) with the slow motional component of the composite spectra above the glass transition temperature arises from the gel phase, especially so-called tight gel, while the fast component is attributed to the spin probe embedded in sol phase. The contribution of gel phase to the slow component was found to be negligible at higher temperatures, and spectra show the characteristic of spin probe in one motionally homogeneous environment. At low temperature, the ESR spectra approach the rigid limit spectrum, with a characteristic separation between the outer peaks ($2A_{zz}$) of about 70 G. With increasing temperature, the spectral lines narrow and the outer peaks shift inward. Above 333 K, all three peaks are narrow and have the same intensity indicating a higher mobility of the spin probe in the polymer matrix. The presence of broad component above $T_g$ (210 K) can be attributed to the spin probes located in gel regions, in which a number of polymer segments are motionally restricted due to interchain interactions and chain entanglements. The narrow component, characteristics of a polymer above the $T_g$, which originated from the spin probes located in the regions undergoing cooperative molecular motions, started appearing at 260 K Fig. 1(b, c, d and e) shows the ESR spectra of spin probed semi IPNs with different compositions (b-35, c-50 PMMA wt.%), crosslink density (c-2% & d-4%) and molecular weight (semi IPN - e, low molecular wt. PI). Spectra in the low temperature region are similar to the spectra of pure spin probed PI. The spectra of semi IPNs at higher temperatures show a central line of higher amplitude when compared to pure PI spectra, suggesting a dynamic anisotropic state of rotation. In the range 293–390 K, the spectra are composed of two components differing in their outer peak separation and line shapes. These two spectral components corresponds to spin probes embedded in two different motional environment; an indication of microphase separation. The plot of $2A_{zz}$ vs temperature for spin probed semi IPNs is shown in Fig. 2. The extrema separations at low temperature are similar. However, at a characteristic temperature $T_h$, the outer peaks splitting decreases strongly with increasing temperature. This transition is shifted to higher temperatures with increasing PMMA content in the system. This effect reflects the decreased mobility when the concentration of PMMA increases and is in good agreement with the DMA observations (Fig. 8). The difference in variation of extrema separation of semi IPNs with temperature suggests that the probe is sensitive to composition variations and this explains the presence of two spectral components in spin probed semi IPNs.

Dynamic heterogeneities observed in semi IPNs are characteristics of systems with two $T_g$'s corresponding to each component. The slow motion component is predominantly connected with spin probes embedded in phase resembling restricted molecular motion of the PMMA and polyisoprene chains close to rigid PMMA chains. The narrow component is due to the spin probes located in the mobile PI phase and flexible PMMA chains. The outer extrema separation $2A_{zz}$ is significantly reduced with increasing temperature, indicating a higher mobility of the spin probe in the polymer matrix. At higher temperatures, the mobility of probe molecules in each component becomes comparable and only fast motional spectra are obtained. The observation of two components in all semi IPNs indicates dynamically different molecular environments due to local composition fluctuations. However this should not be taken as an evidence for only two discrete dynamic states. More likely, the system has a range of chain dynamics centered on the two types of sites detected in ESR experiments. This explains the broadening of two $T_g$'s of semi IPNs in DMA analysis (Fig. 8).

In the range 293–363 K, the PI matrix is above its $T_g$, such that its main chain and segments are motionally active and contribute to the narrow component in the spectra. As the temperature increases, the main chain and segmental motions increases which induces high free volume in the matrix. Higher rates of rotational motion of the probe at high temperatures are due to the generation of larger free volume and increased mobility of the polymer segments. The PMMA domains in the above said temperature ranges are far below its $T_g$ and only side chain groups motions are active at lower temperatures.

ESR spectra for semi IPN with 35 wt-% PMMA showed a complex spectra with narrow component started appearing at 293 K. For

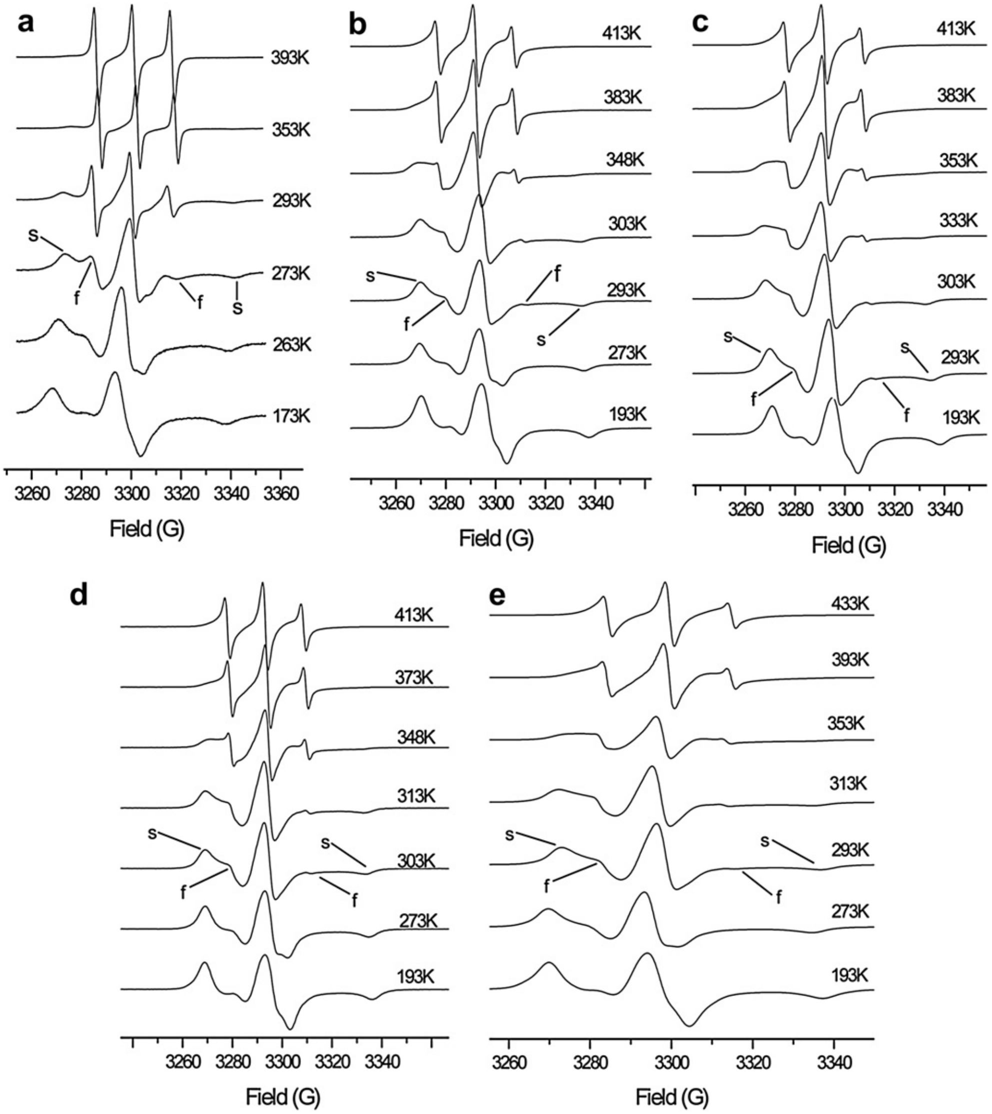

**Fig. 1.** ESR spectra of probe measured as a function of temperature in a: PI, b: semi IPN with 35 wt-% of PMMA, c: semi IPN with 50/50 comp., d: semi IPN 50/50 with highly crosslinked PI, e: low mol. wt. PI semi IPN 50/50 composition.

pure PI, narrow component starts appearing around 268 K. Here comes the significance of ESR spectroscopy as a potential tool that allows a close look into structural and dynamic heterogeneities in multicomponent polymer systems, on a length scale too small (<5 nm) to be observed by differential scanning calorimetry (DSC), dynamic mechanical analysis (DMA) or electron microscopy. IPN synthesis is considered as an easy way to introduce some degree of phase mixing between two incompatible polymers. The shifting of the appearance of narrow component to higher temperature is an indication of the degree of interpenetration of rigid PMMA chains into highly mobile PI chains. The presence of rigid PMMA chains stiffens nearby highly mobile PI chains and imparts restrictions on its motional behavior. This give rise to dynamic heterogeneities within the PI matrix. The PI chains located far from PMMA chains are undergoing molecular motions above its $T_g$ and those close to or intimately mixed with rigid PMMA chains are subjected to restricted molecular motion which resulted in the observed shift. SEM (Fig. 11) and TEM pictures of this same composition shows that PMMA domains are highly dispersed throughout the PI matrix with domain size ranges between 40 and 70 nm; an indication of enhanced mixing [19]. Therefore high temperature is needed to overcome the motional restrictions imparted by the interpenetration of PMMA chains. This shift of transition $T_h$ to higher temperature as a result of enhanced mixing is also detected in DMA experiment (Fig. 8) as a slight inward shift along with the appearance of a shoulder in high temperature side of PI transition. Moreover, DMA analysis showed that both phases seem to have more interaction between each other at this particular composition. The characteristic molecular architecture developed during IPN synthesis such as permanent physical entanglement of chains of both components, and penetration of PMMA chains into entangled PI network, contributes to the need for the requirement of higher temperature for the narrow component to be observed in the ESR spectra. The intensity of narrow component at higher temperatures is less when compared to the pure PI. This also signifies the interaction and cooperative motional behavior of both components at higher temperature. It should be noted that these noticeable changes in spectra are observed well above $T_g$ of PI. Even though there are no noticeable changes in spectra in the glass transition region of PI (205–215 K), the measurement of rotational

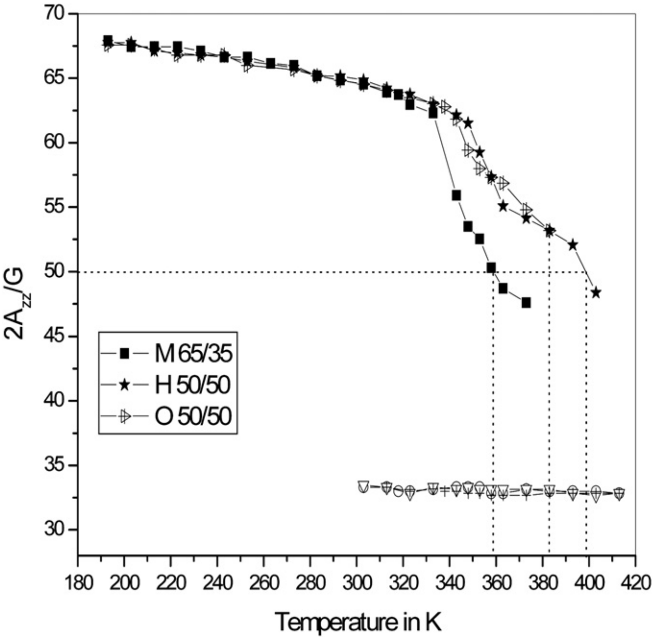

**Fig. 2.** Outer extrema separation (2Azz) vs temperature for different semi IPNs.

correlation times detected the distinct motional region associated with the α-relaxation of PI and this will be discussed later.

The broad component arising from the motionally restricted regions in semi IPNs mainly reflects the motional behavior of PMMA chains in highly mobile PI matrix. The close proximity and mixing of highly mobile PI chains with PMMA chains induce some flexibility in rigid PMMA chains. Therefore PMMA chains located in PMMA rich and PI rich domains have different motional characteristics. The PMMA domains intimately mixed with PI chains reach the cooperative segmental motion at a lower temperature than those located in PMMA rich regions. The broad component almost disappears around 390 K and spectra measured above this temperature show a fast motion of nitroxide radical with enhanced freedom. We assume that majority of spin probes are located in highly continuous PI matrix when compared to highly dispersed PMMA domains. Therefore, probes located in the PI phase have a major share in the overall contribution to the observed ESR spectra. If we assume that the contribution from the gel regions of PI matrix is negligible at high temperature, then taking into account the concentration of PMMA, its dispersed morphology and spin probe distribution in the IPN, the strong intensity of broad component at 348 K could have occurred by some contribution from PI phase also in addition to the major share from PMMA domains. This indicates that PI chains lying in close proximity to PMMA chains are stiffened to some degree, which in turn results in dynamic heterogeneity within PI and PMMA phases. This explains the ESR observation of the shift of $T_h$ to higher temperature and a strong broad component which are in good agreement with DMA observation for this particular semi IPN. Fig. 9 shows the α-relaxation of this semi IPN. A shift and broadening of $T_g$'s are considered as an indication of phase mixing and dynamic heterogeneity. In this case, the transition corresponding to PI in semi IPN is slightly shifted to higher temperature when compared to pure PI. This is a clear indication of the stiffening of PI matrix. Also a shoulder can be seen at the high temperature side of the PI transition which clearly shows the dynamic heterogeneity introduced in PI phase due to the presence of PMMA chains.

In the semi IPN with 50 wt-% PMMA (Fig. 1c), the low temperature spectra are similar to those of pure PI and the fast component starts appearing at 293 K. Both slow and fast components are present up to 400 K and above that temperature the mobility of the probe molecules in each component becomes comparable and only fast motional spectrum is obtained. In low molecular weight semi IPN with 50/50 composition (Fig. 1e), fast component starts appearing at 293 K. Low molecular weight of PI allows both components to mix effectively which mutually influences the mobility of both chains. The slow component is present up to 423 K and above that we see an isotropic spectrum. Also the percentage of fast component is lower when compared to all other semi IPNs studied. We will provide an explanation for this later. In highly crosslinked semi IPN with 50/50 composition (Fig. 1d), the fast component starts appearing at 303 K. Here $T_h$ is shifted to higher temperature with increase in crosslink density. Crosslinking is expected to restrict the chain mobility and suggests that the reduced dynamics of the polymer matrix hinders the formation of concentration fluctuations, and a higher temperature is needed in order to obtain the concentration inhomogeneity necessary to observe two types of the nitroxide mobility in the ESR spectra. In DMA analysis, the α-relaxation of PI shows a slight shift to higher temperature for the highly crosslinked semi IPN when compared to the less crosslinked semi IPN of the same composition (Fig. 1c), which is in good agreement with the ESR result.

### *3.2. Spectral simulations and line shape analysis*

Spectra at high temperature give some interesting information which can be correlated with the influence of crosslink density on the morphology obtained by comparing with DMA, SEM, and TEM results. For this purpose we compared and simulated all the spectra obtained at 363 K for PI and semi IPNs. To determine the relative populations of rigid and mobile components, the ESR spectra were simulated using spectral fitting program NLSL which is based on Stochastic Liouville equation (SLE) and utilizes modified Levenberg–Marquardt minimization algorithm to calculate the best fit with experimental spectra [20]. The spin probe motion was assumed to follow the isotropic Brownian diffusion model. The components of the **g**- and **A**-tensor were determined from the rigid limit spectra. However, in the cases where this was not possible the components of **g**- and **A**-tensor were determined during the fitting procedure. Initial fits were obtained by varying isotropic Gaussian line broadening and rotational diffusion rate parameters for every component. The fits were subsequently refined by varying orienting potential coefficients. The quality of fit was determined by correlation coefficient, *r*, which varied from 0.996 to 0.998. The simulated spectra of semi IPNs at 363 K are given in Fig. 3 (dotted line). The parameters used for the multicomponent ESR spectral fitting are given in Table 1. gxx, gyy and gzz are Cartesian components of the g-tensor for the electronic Zeeman interaction, axx, ayy and azz are Cartesian components of the electron/nuclear hyperfine tensor in Gauss, gib0 represents isotropic Gaussian line broadening, rbar is the logarithm of the "average" rotational diffusion rate in $s^{-1}$ and the c20, c22, c40, c42 and c44 are the orienting potential coefficients. The quantitative estimations of the slow and fast components in the semi IPNs and pure PI as well as the corresponding rotational correlation times are given in Table 2.

The homopolymer PI shows a very narrow spectrum with the maximum amount of fast component (43.8%) among all of the studied samples. All the semi IPN spectra show the peculiarity of the presence of slow component in it. As we discussed, the semi IPN with 35 wt-% of PMMA shows the characteristics of a highly dispersed phase morphology with the PMMA chains closely penetrating into the PI matrix. This particular composition (65/35)

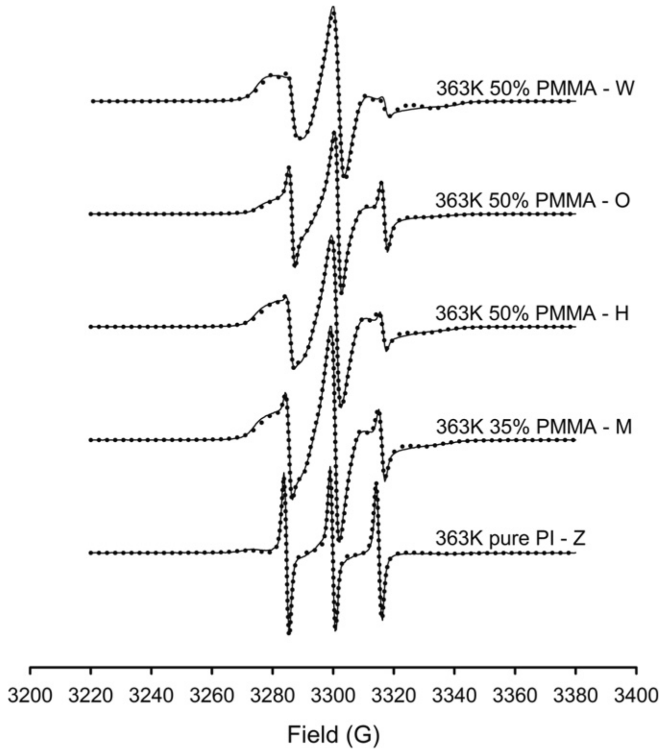

**Fig. 3.** Simulations and comparison of ESR spectra of all semi IPNs at 363 K.

**Table 2**
Quantitative estimation of slow and fast components and calculation of correlation times by simulation of spectra at 363 K.

| Sample | Slow component | | Fast component | |
|---|---|---|---|---|
| | Amount/% | $\tau_R$/ns | Amount/% | $\tau_R$/ns |
| W-50% PMMA | 92.9 | 8.12 | 7.1 | 0.44 |
| O-50% PMMA | 81.5 | 5.50 | 18.5 | 0.27 |
| H-50% PMMA | 87.4 | 7.01 | 12.6 | 0.48 |
| M-35% PMMA | 83.7 | 5.37 | 16.3 | 0.53 |
| Z-0% PMMA | 56.2 | 5.36 | 43.8 | 0.25 |

showed maximum miscibility among all the semi and full IPNs studied (full-IPN ESR article in preparation). The spectra of highly crosslinked semi IPN with 50/50 composition (O) shows a larger amount of fast component (18.5%) when compared to that of less crosslinked, 65/35 PI/PMMA semi IPN (16.3%). Both of these semi IPNs have the same morphology. This unusual behavior is resulted from the effect of miscibility.

The ESR observation confirms the degree of maximum miscibility at the concentration of PMMA less than 35 wt-%. The spectral behavior shows that the influence of miscibility surpasses the crosslinking effect. As a result, the highly mobile PI chains become slightly rigid and have restricted motion at concentration of PMMA less than 35 wt%. The effect of miscibility prevents the highly mobile PI chains from achieving higher mobility and imparts restricted molecular motion. This leads to the low percentage of mobile component in semi IPN with 35 wt% of PMMA when compared to that of 50/50 semi IPN at the same temperature. This difference is more pronounced in the spectra obtained for both semi IPNs at 348 K (Fig. 1b and d). The 65/35 PI/PMMA semi IPN sample showed a shift in the α-relaxation of PI to a higher temperature and the relaxation is also broadened with the appearance of a shoulder in the high temperature side of PI transition. The broadening of PI relaxation in the 65/35 semi IPN is far more pronounced at the higher temperature side than those of highly crosslinked (4–50/50) semi IPN. More importantly, this particular semi IPN was found to form a strong interphase from which the shoulder arises in PI relaxation. This means that the 65/35 semi IPN matrix is more stiffened than the other and this is what we observed in the ESR analysis. In the highly crosslinked semi IPN with 50/50 composition (sample O) the ESR spectra shows a considerable decrease in contribution from the rigid phase with an increase in narrow component. The increased crosslink density was found to enhance mixing between the two phases. This enhanced mixing between two chains induce some flexibility in the highly rigid PMMA chains and some PMMA chains starts moving along with the PI chains at this temperature. Enforced miscibility due to heavy crosslinking results in smaller PMMA domains and consequently in a more continuous PI matrix. SEM and TEM pictures (Figs. 11 and 12) reveal smaller domain size for PMMA (around 40 nm) with PI phase more continuous than in the less crosslinked sample [19]. DMA analysis of these samples in Fig. 8 shows an inward shifts in the α-relaxations of PI and PMMA as a result of phase mixing due to the higher crosslinking in PI phase. This higher continuity in PI phase, along with flexibility induced in PMMA chains, lead to the increase in narrow component in highly crosslinked semi IPN when compared to the less crosslinked semi IPN.

ESR spectra of semi IPNs with 50/50 composition (sample H) show complex spectra with still a considerable proportion of spin probe motion arising from PMMA rich domains located in highly mobile environment (slow component 87.4% and fast component 12.6%). For this to happen, the PMMA domains has to be considerably large and the probe must go deep into the domains. Lower crosslinking and higher PMMA content facilitated the development

**Table 1**
Parameters used for the multicomponent ESR spectral fitting.

| Param. | W-50% | | H-50% | | M-35% | | O-50% | | Z | |
|---|---|---|---|---|---|---|---|---|---|---|
| | slow | fast | slow | fast | slow | fast | slow | fast | slow | fast |
| gxx | 2.0085 | 2.0085 | 2.0085 | 2.0085 | 2.0085 | 2.0085 | 2.0085 | 2.0085 | 2.0085 | 2.0085 |
| gyy | 2.0059 | 2.0059 | 2.0059 | 2.0059 | 2.0059 | 2.0059 | 2.0059 | 2.0059 | 2.0059 | 2.0059 |
| gzz | 2.0021 | 2.0021 | 2.0021 | 2.0021 | 2.0021 | 2.0021 | 2.0021 | 2.0021 | 2.0021 | 2.0021 |
| axx | 6.71 | 6.71 | 6.24 | 6.24 | 6.24 | 6.24 | 6.71 | 6.71 | 6.71 | 6.71 |
| ayy | 6.51 | 6.51 | 7.92 | 7.92 | 7.92 | 7.92 | 6.51 | 6.51 | 6.51 | 6.51 |
| azz | 33.64 | 33.64 | 34.20 | 34.20 | 34.20 | 34.20 | 33.64 | 33.64 | 33.64 | 33.64 |
| gib0 | 2.797 | 2.398 | 1.808 | 0.046 | 0.800 | 0.227 | 2.141 | 1.577 | 1.473 | 1.473 |
| rbar | 7.3122 | 8.5777 | 7.3764 | 8.5408 | 7.4917 | 8.4948 | 7.4813 | 8.7886 | 7.4928 | 8.8261 |
| c20 | −0.205 | −0.120 | −0.233 | −1.511 | −0.103 | −0.954 | −0.090 | −0.562 | −0.014 | −0.119 |
| c22 | −0.096 | 0.345 | −0.141 | −0.057 | 0.040 | −0.166 | −0.294 | −0.003 | −0.789 | −0.617 |
| c40 | −0.408 | 0.964 | −0.473 | −1.452 | −0.097 | −1.876 | −0.389 | −0.230 | 1.080 | −1.461 |
| c42 | 0.011 | 0.189 | 0.176 | 3.330 | 0.462 | 2.241 | 0.303 | 2.657 | −1.349 | 1.593 |
| c44 | −0.257 | 0.179 | −0.598 | 0.037 | −0.027 | 0.762 | 0.000 | 0.000 | 0.000 | 0.000 |

of larger PMMA domains in this semi IPN. DMA, SEM (Fig. 11c), and TEM analysis [19] show that at this composition PMMA phase was in a transition zone between nodular structure (large domains) and dual phase morphology with PI phase still maintaining to form the matrix. The low molecular weight semi IPN with 50/50 composition shows major contribution from rigid component (92.9%) even at higher temperature unlike other semi IPNs. Here the ESR spectral line shape and simulation data reflects the continuity of the phases in semi IPNs. SEM analysis shows that PMMA phase is more continuous than PI phase for this semi IPN when compared to other semi IPNs (Fig. 11e). So this semi IPN maintains the rigid nature at higher temperature giving rise to the observed broad spectrum. Therefore, we propose that the shape of the ESR spectrum and simulation data can be used to arrive at some morphological conclusions with the help of other techniques like DMA, SEM, and TEM, given that one of the components should be elastic and other a rigid polymer. The correlation times ($\tau_c$) calculated from the simulations (Table 2) were in good agreement with the results obtained by ESR and DMA measurements. The correlation time of the fast component in 65/35 semi IPN (M) was found to be higher than the correlation times of all other semi IPNs. This proves the stiffening of the PI matrix due to the presence of PMMA since the fast component was mainly arising out of PI phase. Sample W showed the highest value for the slow component which was also consistent with the results obtained in our analysis.

### 3.3. *Dynamics of PI/PMMA semi IPNs from correlation times*

The best method to calculate the correlation times is by spectral simulations. An alternative method that allows a reasonable estimate of correlation time can be obtained from the temperature dependence of $2A'_{zz}$ [9,11]

$$\tau_c = a(1-S)^b \tag{1}$$

the ratio $S = 2A'_{zz}/2A_{zz}$ is calculated based on rigid limit value $2A_{zz}$ measured at 100 K. Brownian diffusion model was used for the present study and an intrinsic line width of 8 G was calculated from the simulation of rigid limit spectra for semi IPN at 100 K. For these conditions, the values of a and b are $1.10 \times 10^{-9}$ and $-1.01$, respectively. The correlation times in the high temperature regime can be calculated from equation [9,11]

$$\tau_c = 0.65 \times 10^{-9} \Delta B \left( \left[ \frac{I(0)}{I(-1)} \right]^{1/2} + \left[ \frac{I(0)}{I(+1)} \right]^{1/2} - 2 \right) \tag{2}$$

where I(−1), I(0) and I(+1) are intensities of low, central and high field lines, respectively, and ΔB is the line width of central line. The $\tau_c$ calculations were performed for both fast and slow motional regions. For the slow motional region, $\tau_c$ was estimated from equation (1) up to a temperature where S is undefinable, since the outer lines begin to converge to the motionally narrowed spectrum and $\tau_c$ values of slow and fast component became almost undistinguishable. Equation (2) for fast motional region was used to calculate the $\tau_c$ from the temperature at which the ESR spectrum showed relatively sharp hyperfine lines, up to 413 K [21].

Arrhenius plots of $\tau_c$ are shown in Fig. 4 (a, b, c, and d). Several motional regimes can be seen for semi IPNs in the temperature range of 193 K–413 K. Four crossover points for sample M, three for samples H and O and one for W can be seen. The existence of several crossover points can be explained as follows. The low temperature (193 K–233 K) and high temperature (348 K–393 K) crossover points coincides with the glass transitions of PI and PMMA respectively for all semi IPNs (Sample W does not show the distinct motional regime associated with $T_g$ of PI phase. We found that the nature of probe motion is strongly influenced by the molecular motions associated with PMMA segments because the rigid phase was found to be more continuous in this case). The activation energies ($E_a$) determined in the glass transition region of PI were found to be the same within the experimental uncertainty, for all samples we examined. $E_a$ (low temp) = 15.0 ± 2 kJ/mol. This confers that regardless of the model used in the calculation of correlation times, the molecular motions of the probe are activated by the same molecular process. Though the activation energies are much lower compared to values usually observed in the glass transition region, we suggest that the observed dynamics is correlated to the α-relaxation of PI, because the position of this motional regime, as shown in figures (Fig. 4), follows the same trends of shifts in position of α-relaxation of PI as observed in DMA analysis. The motional region associated with the α-relaxation of PI was found to be shifted to higher temperature in the case of 65/35 semi IPN when compared to others and this is in exact agreement with the DMA observation for this semi IPN.

The activation energy ($E_a$) in the region 243 K–313 K was found to be 9 ± 2 kJ/mol, same for all semi IPNs. The value agrees with the values reported earlier for similar systems [8]. Here the probe is at a temperature below $T_g$ of PMMA and is activated by local relaxation modes in the polymer matrix. In general, such sub $T_g$ relaxations have very small activation energies [8]. The activation energy for the high temperature regime was found to be 48 kJ/mol, 56 kJ/mol, 68 kJ/mol and 35 kJ/mol for M, H, O and W semi IPNs, respectively, within the experimental uncertainty. The higher value compared to the low temperature region is in good agreement with the previous studies reported [8,9]. Among the three semi IPNs studied, the 65/35 sample and low molecular weight semi IPN showed the lowest activation energy because of the flexibility induced in PMMA chains by the highly mobile PI chains during IPN formation. This is the result of phase mixing which is evident in the shift and broadening of the relaxation curve in DMA scans. Since the activation energy shows a trend that can be correlated to the level of mixing between PI and PMMA chains, we suggest that the probe mostly reflects the motional characteristics of interface regions. Low activation energy is needed for those PMMA chains that are intimately mixed with the highly mobile PI chains. Even though the activation energies are much lower than compared to the values usually observed in the glass transition region (200–400 kJ/mol), we suggest that the motional characteristics of probe in this region is correlated to the α-relaxation of PMMA, because we found that $T_{50G} \approx T_g$ for the rigid component (Fig. 2). For this to happen, the probe should be part of the PMMA segment whose motion is activated at $T_g$.

### 3.4. *Correlation between $T_{50G}$ and $T_g$*

The $T_{50G}$ is defined as the temperature where the separation of the outermost peaks ($2A_{zz}$) in the ESR spectrum of the nitroxide radical in the polymer matrix is 50 G. Several authors have suggested that $T_{50G}$ is a high frequency glass transition. Because the rotational frequency at $T_{50G}$ is $\sim 5 \times 10^8$ Hz for nitroxides, $T_{50G}$ is normally higher than the $T_g$ normally measured at a frequency of ∼1 Hz. $T_g$ reflects the macroscopic character of segmental mobility of polymers, while $T_{50G}$ gives purely microscopic information through the mobility of spin probes.

$T_{50G}$ corresponding to the broad component was found to indicate the $T_g$ of PMMA in semi IPNs (Fig. 2). Considering the broad nature of $T_g$'s observed in semi IPNs by DMA analysis and different methodology used in ESR, the $T_{50G}$ values obtained falls within the range of error limit of less than 8°. For semi IPN with 50/50 composition (sample H), the $T_{50G}$ of rigid component falls exactly in the region of main relaxation of PMMA ($T_{50G} \approx T_g \approx 399$ K). Low

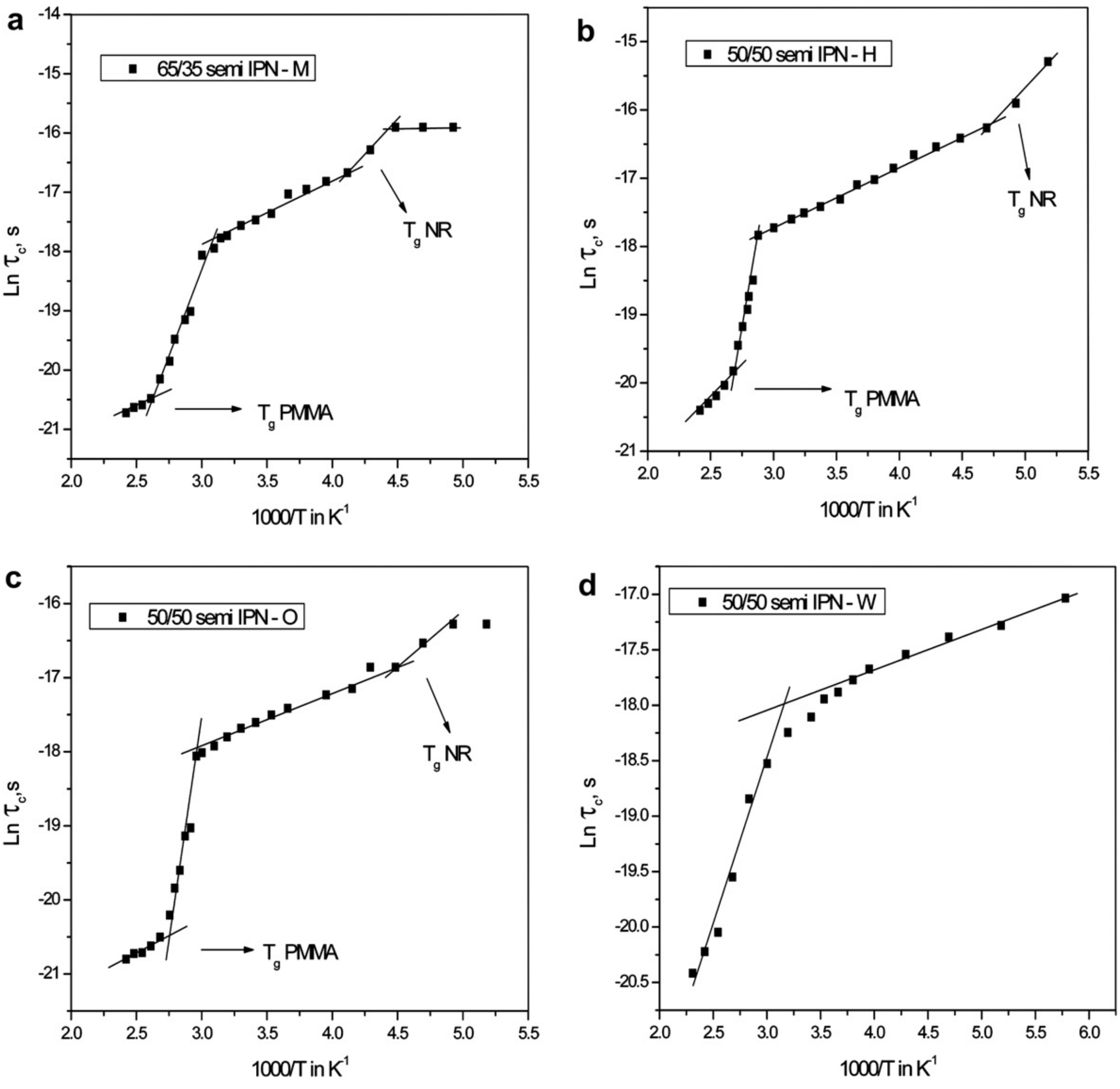

**Fig. 4.** Correlation times and different motional regions in semi IPNs (a) sample M – 65/35, (b) sample H – 50/50, (c) sample O – 50/50, (d) sample W – 50/50.

molecular weight semi IPN – W also showed the same observation as above. In the case of highly crosslinked semi IPN with 50/50 composition (sample O), $T_{50G}$ value was found to be shifted to lower temperature (385 K), which is in good agreement with the inward shifting of $T_g$ observed in DMA analysis. The high temperature region seems to reflect the glass transition temperature, because we found that $T_{50G} \approx T_g$. We can therefore assume that the probe is part of the polymer segment whose motion is activated at $T_g$ and the probe explores a space that is roughly equal to this polymer segment. Based on the free volume treatment of Bueche, Kusumoto et al. suggested the below equation [8,9].

$$T_{50G} - T_g = 52\left[2.9f(1 - \ln f) - 1\right] \quad (3)$$

for calculating the ratio $f$ = V (probe)/V (segment). In our case $T_{50G} \approx T_g$ and we obtain $f = 0.1$. The volume of the label is 170Å$^3$. This result indicates that the volume of the PMMA segment undergoing glass transitional motion is 1700Å$^3$ (1.7 nm$^3$).

### 3.5. C-13 $T_{1\rho}$ relaxation time

The C-13 $T_{1\rho}$ relaxation times, unlike the corresponding proton $T_{1\rho}$ times, are not influenced by spin diffusion, and therefore the relaxation of each carbon can be followed. In the $T_{1\rho}$ pulse sequence, a carbon magnetization is built-up via cross-polarization and the carbons are held in the rotating frame without direct contact with the proton reservoir for a variable period τ, allowing the C-13 polarization to decay in its own rotating field. This structure of the pulse sequence results in sensitivity of $T_{1\rho}$ to molecular motion in the 10–100 kHz frequency range, characteristic for the relatively long-range cooperative motions of a polymer chain below the glass transition. The C-13 $T_{1\rho}$ relaxation is the sum of spin-lattice and spin–spin relaxation processes. The spin–spin processes generally become significant in determining the C-13 $T_{1\rho}$ of the highly crystalline polymers [14]. Schaefer et al. have concluded that in glassy polymers, the spin-lattice component is dominant and that the C-13 $T_{1\rho}$ is predominantly determined by motional processes, for spin-locking frequencies greater than 30 kHz [13,22]. There is a large body of evidence in the literature to show that C-13 $T_{1\rho}$ is dominated by spin-lattice processes in amorphous polymers in both glassy and rubbery states [14,22,23]. Therefore, the C-13 $T_{1\rho}$ relaxation times can be effectively utilized to investigate the motion of PMMA chains in homopolymer and in semi IPNs below glass transition temperature. The carbon resonance intensity decays with a time constant equal to the $T_{1\rho}$ by an exponential function:

$$M(\tau) = M(0)\exp(-\tau/T_{1\rho}) \quad (4)$$

thus the slope of a logarithmic plot of the magnetization intensity, M ($\tau$), vs delay time, $\tau$, yield $T_{1\rho}$ value. C-13 NMR spectrum of semi IPN is shown in Fig. 5. Signal from the PI phase could not be followed because of the very low intensity. This happens due to the low dipolar coupling in the highly mobile PI phase and thus cross-polarization will not be effective. The C-13 $T_{1\rho}$ of PMMA homopolymer and two semi IPNs are shown in Table 3. PMMA shows only one motional component for all the carbon atoms, typical behavior of a homogeneous polymer. The fast relaxation of quaternary carbon atom compared to other carbon atoms is an established fact [13]. The PMMA carbon atoms in semi IPNs show two motional components, short and long, except for quaternary carbon atom. The motional heterogeneity observed in PMMA chains of semi IPNs can be directly correlated to the molecular level interactions and mixing occurred with highly mobile PI chains during semi IPN formation. This is also an indication of phase separation. The short and long relaxation components can be attributed to those arising from PMMA rich and PI rich regions. C-13 $T_{1\rho}$ shows that the carbonyl carbon and the ester carbon show enhanced mobility and interaction upon mixing with PI chains, which lead them to relax slowly.

Fig. 6 shows two motional components from the carbon magnetization decay of carbonyl carbon of PMMA in semi IPN. The $-CH_3$ group attached to quaternary carbon enjoys more rotational freedom in semi IPNs than in homopolymer. All the above differences in motional behavior of carbon atoms attached to quaternary carbon atom might have contributed to slight increase in the relaxation time of quaternary carbon atom in semi IPNs. The above observation implies that the semi IPN formation affects the local motions of the individual polymer side chains, as these motions are sensitive to the details of the local environment and packing of the polymer chains.

**Table 3**
C-13 $T_{1\rho}$ relaxations of PMMA and semi IPNs.

| Sample | 182 ppm | | 57 ppm | | 51 ppm | | 23 ppm | |
|---|---|---|---|---|---|---|---|---|
| (40 kHz) Rf | short ms | long ms | short ms | long ms | short ms | long ms | short ms | long ms |
| PMMA | 4.14 | | 2.16 | | 1.49 | | 2.15 | |
| $^{2}NRM_{50}$ (H) | 3.39 | 17.98 | 4.45 | 16.14 | 4.14 | | 4.35 | 9.02 |
| $^{4}NRM_{50}$ (O) | 2.46 | 26.21 | 3.14 | 11.28 | 3.65 | | 2.94 | 7.99 |

Superscript 2 & 4 represents the crosslink density and subscript 50 shows the PMMA content.

### 3.6. Two dimensional WISE NMR

The wideline Separation (WISE) NMR spectroscopy is used to measure the dynamics of solid polymers by correlating the proton line shape with carbon chemical shift. This experiment yields information about dynamics by measuring the degree to which the proton line shapes are averaged by molecular motion. The proton lines are broadened in solids by hetero- and homo-nuclear dipolar interactions. Motionally averaged line shapes are also observed if the atom experiences large amplitude fluctuations that are fast on the time scale of dipolar line widths (50 kHz). The WISE experiment does establish a correlation of the chemical structure and segmental mobility as reflected in the C-13 chemical shifts and the H-1 line shapes, respectively. Fig. 7 shows contour plots of the WISE NMR spectrum of PI/PMMA 50/50 semi IPN at 298 K. Several well resolved peaks are observed, including the PMMA protons of the $-CH_2-$ group at 50 ppm, $-OCH_3$ at 54 ppm and $-CH_3$ at 27 ppm. From PI phase, proton peaks for $-CH_2-$ at 36 ppm, other $-CH_2-$ at 30 ppm and $=CH-$ group at 129 ppm are clearly resolved. Peaks at 27 ppm contain overlapped peaks from methyl groups in PI and PMMA. The contour plot shows that very different proton line widths are observed for the PMMA and PI chains. It is evident from the contour plot that the line width of PMMA protons at 50 ppm and 54 ppm are much larger than the protons of PI at 36 ppm and 30 ppm. This is the characteristic of a phase separated multicomponent system consisting of rigid and mobile phases. The WISE experiment shows that the protons in the ester group (54 ppm) of PMMA have the highest mobility and $-CH_2-$ protons at 50 ppm are the most rigid among the protons in the PMMA phase. In fact, the

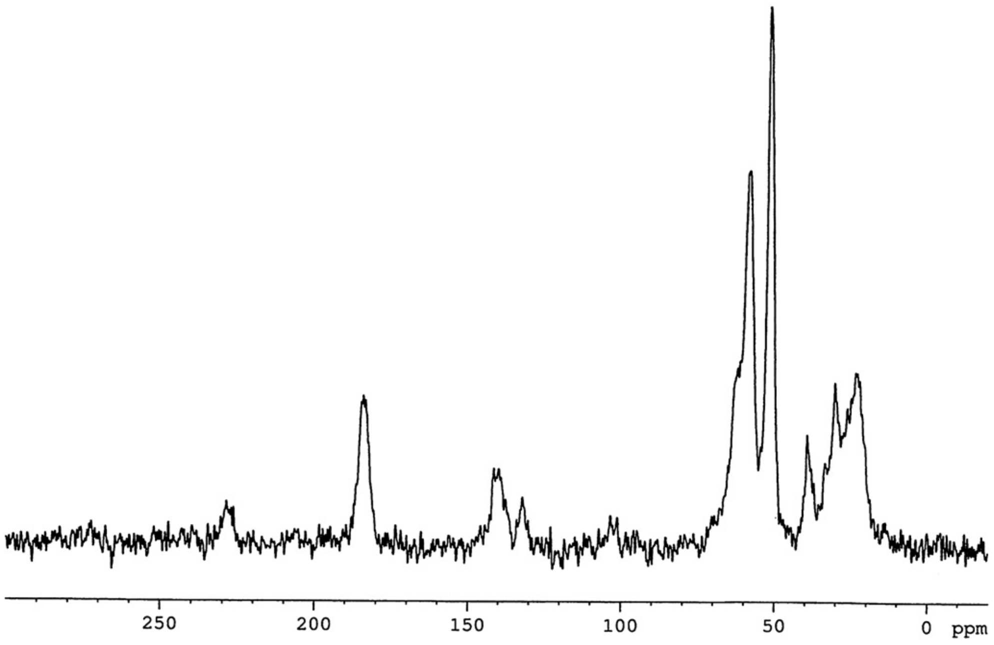

**Fig. 5.** C-13 NMR spectrum of semi IPN – H.

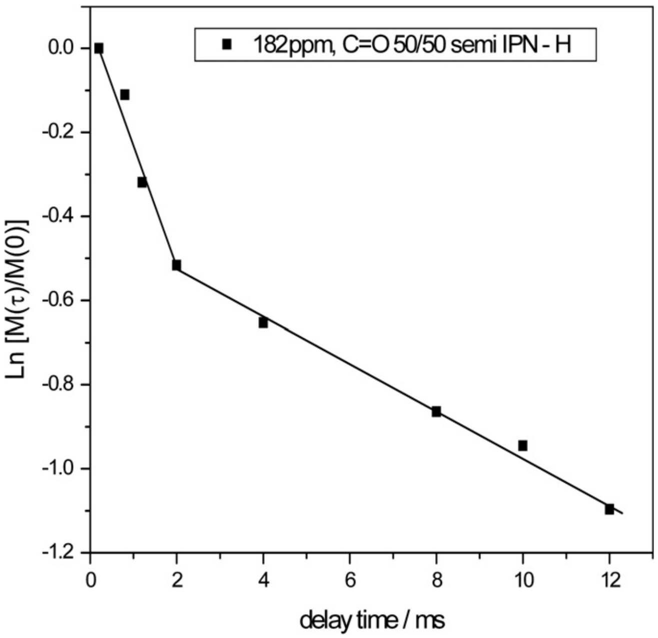

**Fig. 6.** Logarithmic plot of C-13 resonance intensities as a function of delay time for carbonyl group of PMMA in semi IPN.

relaxation measurement showed that the ester group enjoyed enhanced mobility upon mixing with PI chains during semi IPN formation. Contour plots shows that the proton in =CH– (129 ppm) group of PI phase is less mobile than the protons in the ester group of PMMA. Protons in PI chains observed at 36 ppm and 30 ppm are motionally very active when compared to all the other protons in semi IPNs.

### 3.7. Dynamic mechanical analysis (DMA)

Relaxations of semi IPNs and homopolymers are shown in Fig. 8. The α-relaxations of PI and PMMA appear around 201 K and 403 K, respectively. β-relaxation of PMMA can be noticed only for the PMMA homopolymer around 313 K. The main relaxation of PMMA is very weak in 25 and 35 PMMA wt-% compositions. Even though the α-relaxations of PMMA did not show up in the two compositions mentioned above, the presence of PMMA and its impact is revealed in the slight inward shift and broadening of the α-relaxation of PI. In the case of 65/35 semi IPN, a shoulder can be clearly seen at the high temperature side of the α-relaxation of PI (Fig. 9). This effect is more pronounced in the case of full IPNs having the same composition and it will be discussed in a forthcoming paper. This indicates that some of the rigid PMMA chains are in close proximity to highly mobile PI chains to influence the α-relaxation of PI, and this influence can be seen as a slight inward

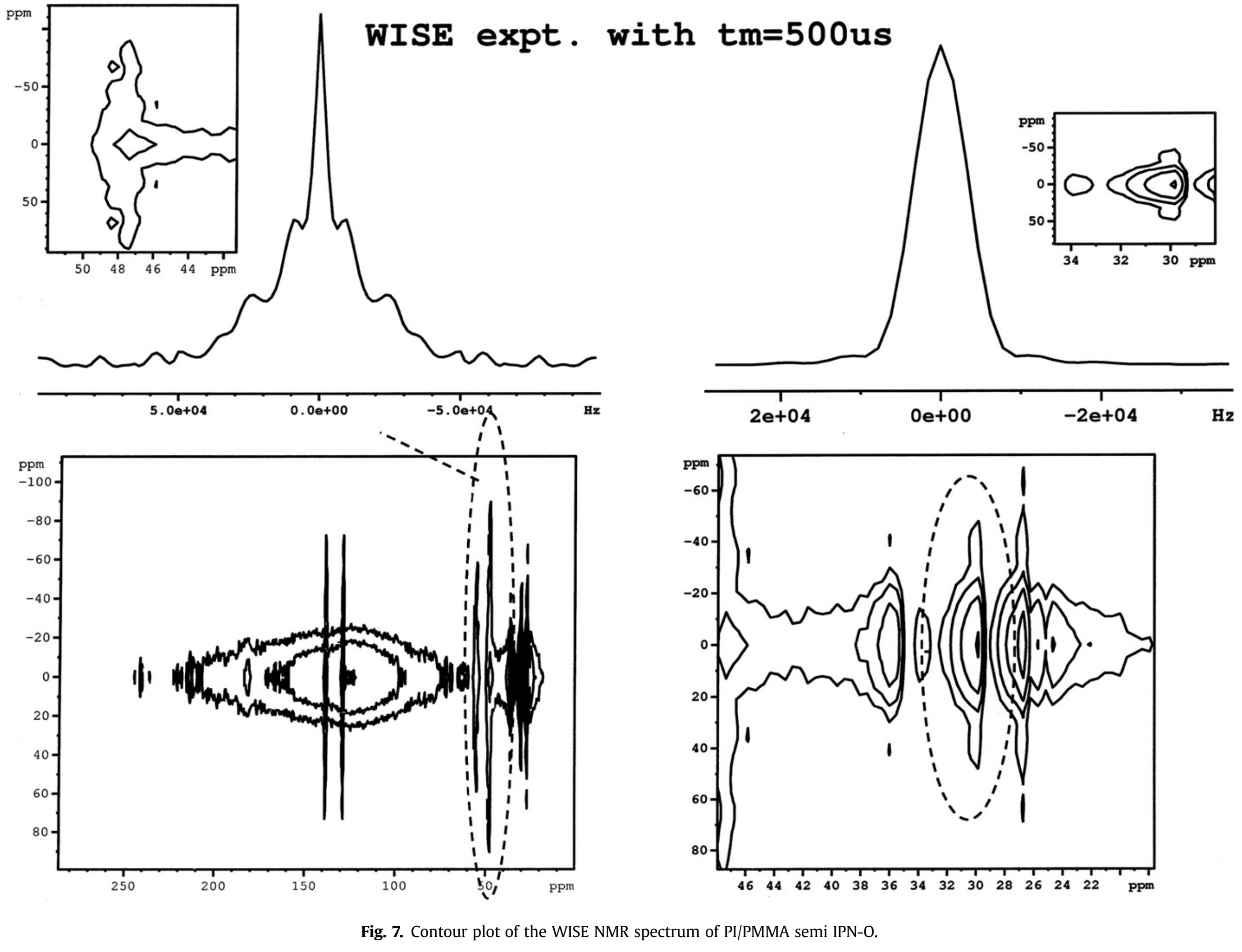

**Fig. 7.** Contour plot of the WISE NMR spectrum of PI/PMMA semi IPN-O.

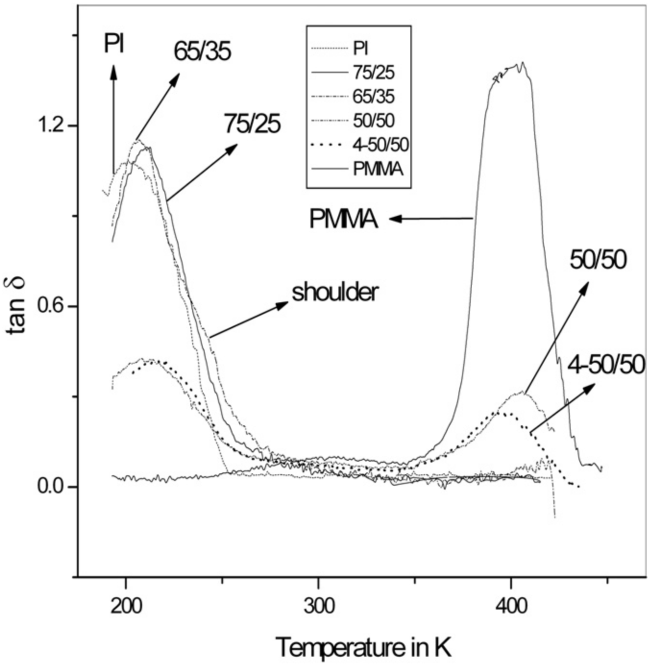

**Fig. 8.** Tan $\delta$ vs Temperature scans of semi IPNs and homopolymers.

shift and as a shoulder in high temperature side of PI relaxation (Fig. 9). The 65/35 semi IPN was found to form a strong interphase between two phases. The morphology of this semi IPN is schematically represented in Fig. 10. The shoulder seen at the high temperature side of PI transition was due to the presence of this strong interphase. The relaxation times of the PI chains will be different for those that are very close and far away from the rigid PMMA chains. This will result in the distribution of relaxation times and leads to the broadening of PI relaxation peak. The broadening is also an indication of the presence of a fluctuation in the local glass transition temperature. Both phases seem to have more interaction between each other at this particular composition.

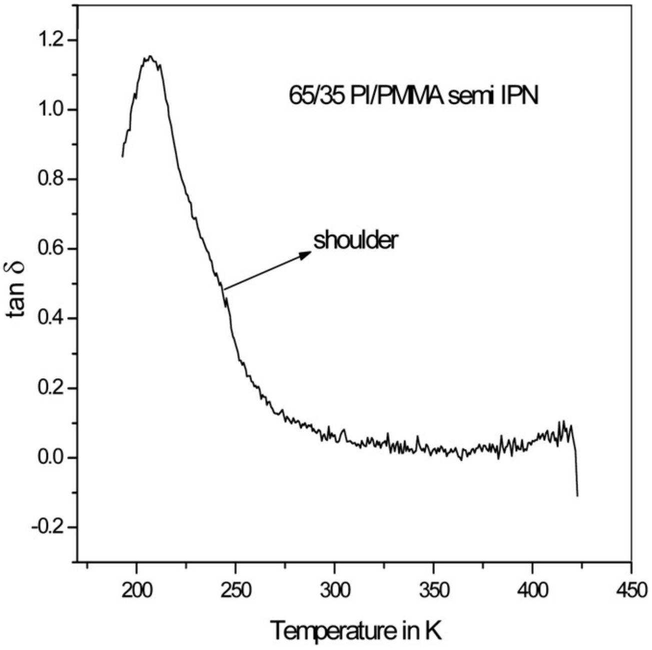

**Fig. 9.** Broadening of the $\alpha$–relaxation of PI in 65/35 semi IPN.

The SEM images (Fig. 11) show the tiny and dispersed nature of the PMMA phase in crosslinked PI matrix at this composition. The ESR analysis also supports the above observation. In 75/25 PI/PMMA semi IPNs, the $\alpha$-relaxation peak of PI is shifted to higher temperature. The PMMA at lower concentration was found to stiffen the highly mobile PI chains. This could not have been possible without certain degree of chain mixing between both components. Therefore, higher temperature is needed to overcome the motional restrictions imparted on PI networks by rigid PMMA chains. When both components are at 50/50 composition, a distinct dynamic mechanical spectrum is obtained. The sharp transitions corresponding to the $\alpha$-relaxations of PI and PMMA are clearly seen in the DMA scans which is a characteristic of immiscible system. Two sharp transitions show the existence of two motionally distinct regions in the semi IPNs. PI relaxation is broader when compared to the homopolymer. The broadening of these relaxations indicates the mutual interaction between the highly mobile PI chains and rigid PMMA chains. Close proximity of PMMA chains imparts some rigidity in highly mobile PI chains. In the same way, the presence of highly mobile PI chains near to PMMA chains reduces its stiffness. This mutual influence affects the relaxation time of each component. Thus a distribution of relaxation results from both components in accordance with the degree of this mutual influence. This explains the broadening of high temperature side of lower transition and low temperature side of higher transition.

In the case of highly crosslinked semi IPN with 50/50 composition, an inward shift of $\alpha$-relaxations is observed in the tan $\delta$ sweep. The slight inward shift of $\alpha$-relaxations of both components is an indication of some degree of phase mixing. As we discussed, the heavy crosslinking in the PI phase resulted in close mixing between the two phases. Mutual influence arising out of close mixing resulted in the strengthening of many of the highly mobile PI chains, and at the same time, some degree of flexibility is also induced in the rigid PMMA chains. This causes many of the PI chains to relax at a higher temperature and most of the PMMA chains to relax at a lower temperature, resulting in the slight inward shifts of both transitions. SEM (Fig. 11d) and TEM images (Fig. 12) of this semi IPN show very small PMMA domains in the range of 60 nm as a result of enhanced mixing during semi IPN formation. This fact supports the inward shift of the main relaxation peaks observed in the DMA scans of this semi IPNs. Higher modulus values showed by this sample and distinct behavior above the $T_g$ of PMMA are strong evidence supporting some degree of phase mixing in this semi IPN [19].

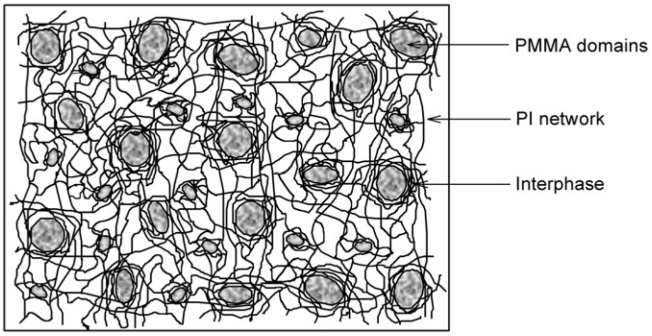

**Fig. 10.** Schematic representation of the morphology of 65/35 semi IPN showing the development of a strong interphase between the nano domains of PMMA and PI matrix.

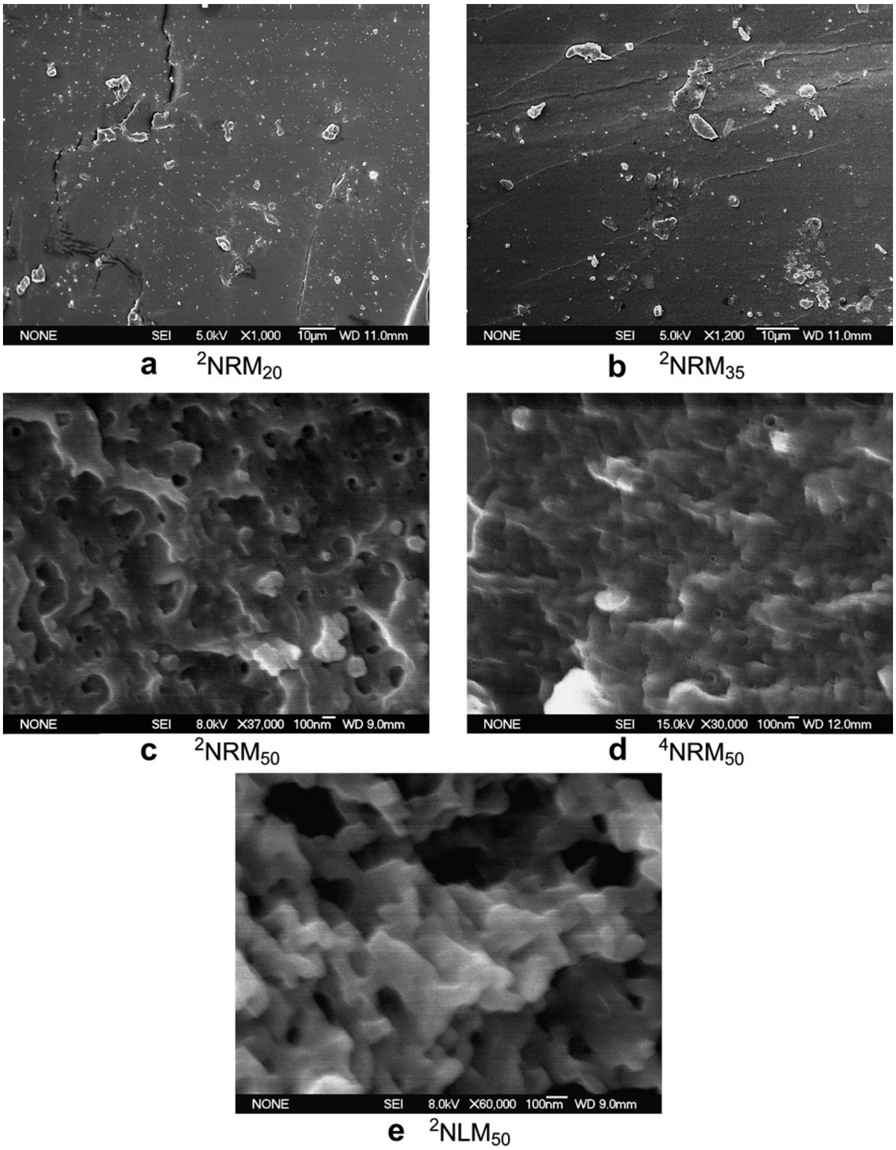

**a** $^{2}NRM_{20}$ **b** $^{2}NRM_{35}$

**c** $^{2}NRM_{50}$ **d** $^{4}NRM_{50}$

**e** $^{2}NLM_{50}$

**Fig. 11.** SEM micrographs of semi IPNs a) 20 wt-% of PMMA, b) 35 wt-% of PMMA c) 55 wt-% of PMMA, d) Highly crosslinked PI (4 wt % of DCP) with 50 wt-% of PMMA e) low molecular weight PI semi IPN (W).

### 3.8. Morphology

SEM images of the semi IPNs are shown in Fig. 11 having PMMA concentrations ranging from 20 wt-% to 50 wt-%. Semi IPNs with low PMMA concentration (up to 40 wt-%) (Fig. 11 a and b) shows a sea-island morphology, and as the concentration increases, a shift to nodular structure morphology can be noticed (Fig. 11c). Semi IPNs showed maximum mechanical performance in this region. When the crosslink density of PI matrix is increased (Fig. 11d), the resulting semi IPN shows a compact structure with small PMMA domains having size in the range of 60 nm. This is the direct result of higher crosslinking of the first formed phase. This nanometer-sized morphology can be clearly seen in the TEM image of highly crosslinked 50/50 semi IPN sample shown in Fig. 12. Morphology of semi IPNs are discussed in more details in another article prepared by the same authors [19]. Low molecular weight semi IPN shows large continuous voids after PMMA is extracted. This supports our ESR observation of the rigid nature shown by this semi IPN due to the more continuous PMMA phase (Fig. 11e).

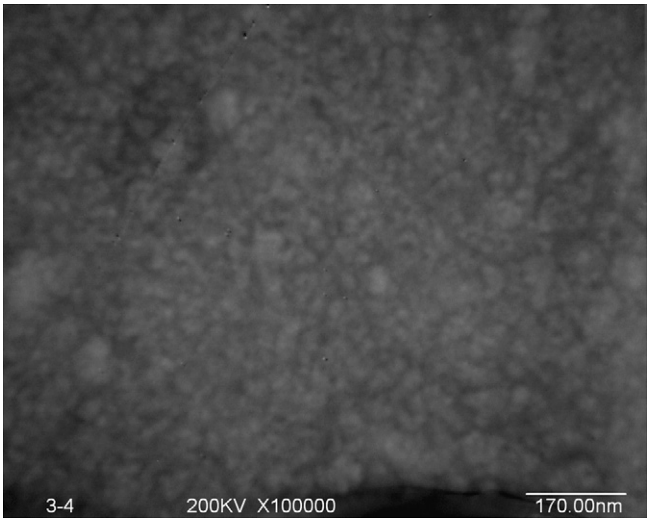

**Fig. 12.** TEM image of highly crosslinked 4 - 50/50 semi IPN (O).

## 4. Conclusions

Main chain and segmental dynamics of PI and PMMA chains in semi IPNs with different composition, crosslink density, and molecular weight were studied in the temperature range of 173 K–413 K, at intervals of 10 K or less, using ESR spin probe technique and dynamic mechanical analysis. The interactions between the two immiscible polymers and the motional behavior of H atoms in the two polymers were analyzed using C-13 $T_{1\rho}$ relaxation measurements and 2D WISE NMR respectively at room temperature. Morphology of the semi IPNs was also investigated by SEM and TEM analysis. The main conclusions from these investigations were as follows:

1. At lower temperatures, the ESR spectra approached the rigid limit spectrum and as the temperature increased, the spectral lines got narrower and outer peaks shifted inward. In the range of 293 K–373 K, a complex spectra were obtained, an indication of the presence of motionally distinct regions in semi IPNs.
2. Semi IPN synthesis resulted in dramatic changes in the motional behavior of both polymers and this was due to the molecular level interpenetration between two polymer chains. The intimate mixing of the rigid PMMA chains with highly mobile PI networks strengthened the PI networks, and this led to the shifting of $T_h$ and α-relaxation of PI to higher temperature in ESR and DMA analyses, respectively.
3. The interchain mixing was found to be more efficient at the PMMA concentration of 35 wt% and resulted in the formation of a strong interphase between the two immiscible polymers. Motional characteristics from these interphase regions contributed to the unusually large slow motional component in the spectra at high temperature (363 K), and also the presence of a shoulder in the higher temperature side of the α-relaxation of PI.
4. Heavy crosslinking in the PI phase resulted in enforced miscibility in semi IPNs. The $T_h$ is shifted to higher temperature and the α-relaxation of both polymers showed a slight inward shift. This enforced miscibility resulted in the development of a nanometer-sized morphology in the same semi IPN.
5. The shape of the ESR spectra and the quantitative estimation of slow and fast components by simulations of spectra were correlated to the morphology of semi IPNs. All the spectra of three semi IPNs with 50/50 compositions were totally different because of the differences in their morphology. It is difficult to arrive at some morphological conclusions from the ESR spin probe spectra; however in this case we have demonstrated the potential of ESR technique in extracting information regarding the morphology such as continuity of phases.
6. Correlation time measurements detected motional regions associated with the low temperature transition of the PI, which is usually hard to determine in conventional ESR experiments. Motional regions associated with the glass transitions of the PI and PMMA were found to follow the same pattern of shifts in α-relaxation of both polymers, as observed in the DMA analysis.
7. The $T_{50G}$ was found to show the $T_g$ of PMMA, and based on the free volume treatment of Bueche, the volume of polymer segments undergoing glass transitional motion was calculated to be 1700 $\text{Å}^3$ (1.7 $nm^3$).
8. Solid state NMR studies also revealed the molecular level interchain mixing between two immiscible polymers in semi IPNs. C-13 $T_{1\rho}$ relaxation revealed that the carbonyl carbon and the ester carbon showed an enhanced mobility and interaction upon mixing with the flexible PI chains. 2D WISE experiment also showed the unusual high mobility in the H atoms attached to the ester carbon, once again proving the influence of highly flexible environment close to PMMA chains.

## Acknowledgements

This study was supported by Department of Science and Technology (DST) (Project no. INT/CROATIA/P-8/05), Government of India and Ministry of Science, Education and Sports of the Republic of Croatia (Project 062-0000000-3209). Prof. Thomas P. Russell, University of Massachusetts Amherst, USA is acknowledged for providing MRSEC facilities in Polymers Science and Engineering Dept. for this research program. The authors also thank Prof. K. V. Ramanathan, NMR Research Center, IISc, Banglore, India for providing experimental facilities. Prof. David E. Budil, Department of Chemistry and Chemical Biology, Northeastern University, Boston, USA is acknowleged for providing ESR spectral simulation program and guidance in simulations. Andrica Lekić, School of Medicine, University of Rijeka, Croatia and Deepak Ninan, University of Massachussets, Amherst, USA, are acknowledged for their help during the course of this research work.

## References

[1] Lipatov YS, Alekseeva TT. Adv Polym Sci 2007;208:1–227.
[2] Babkina NV, Lipatov YS, Alekseeva TT. Polym Sci A 2005;47:2118–23.
[3] Sperling LH. Interpenetrating polymer networks and related materials. New York: Plenum; 1981.
[4] Miwa Y, Drews AR, Schlick S. Macromolecules 2008;41:4701–8.
[5] Miwa Y, Sugino Y, Yamamoto K, Tanabe T, Sakaguchi M, Sakai M, et al. Macromolecules 2004;37:6061–8.
[6] Wolinska-Grabczyk A, Bednarski W, Jankowski A, Waplak S. Polymer 2005;46:2461–71.
[7] Wasserman AM, Yasina LL, Motyakin MV, Aliev II, Churochkina NA, Rogovina LZ, et al. Spectrochemica Acta Part A 2008;69:1344–53.
[8] Muller G, Stadler R, Schlick S. Macromolecules 1994;27:1555–61.
[9] Schlick S, Harvey RO, Alonso-Amigo MG, Klempner D. Macomolecules 1989;22:822–30.
[10] Quo F, Chen S, Peng Z. Mag Reson Chem 2005;43:411–6.
[11] Valić S, Rakvin B, Veksli Z, Grubisić-Gallot Z. Macromolecules 1990;23:5182–6.
[12] Veksli Z, Andreis M, Rakvin B. Prog Poly Sci 2000;25:949–86.
[13] Schaefer J, Stejskal EO, Buchdahl R. Macromolecules 1977;10:384–405.
[14] Jack KS, Wittaker AK. Macromolecules 1997;30:3560–8.
[15] Wu RR, Kao HM, Chiang JC, Woo EM. Polymer 2002;43:171–6.
[16] Schmidt-Rohr K, Clauss J, Spiess HW. Macromolecules 1992;25:3273–7.
[17] Qiu X, Mirau PA. J Mag Reson 2000;142:183–9.
[18] Wagler T, Rinaldi PL, Han CD, Chun H. Macromolecules 2000;33:1778–89.
[19] John J, Nagarajan S, Suriyakala R, Klepac D, Yang W, Valić S, Thomas S, Pius A, submitted for publication.
[20] Budil DE, Lee S, Saxena S, Freed JH. J Magn Reson A 1996;120:155–89.
[21] Grabczyk AW, Bednarski W, Jankowski A, Waplak S. Polymer 2005;46:2461–71.
[22] Schaefer J, Stejskal EO, Steger TR, Sefcik MD, Mckay RA. Macromolecules 1980;13:1121–6.
[23] Schaefer J, Sefcik MD, Stejskal EO, MacKay RA. Macromolecules 1984;17:1118–24.